CRACK GROWTH BEHAVIOR IN RESIDUAL STRESS FIELD IN VESSEL TYPE STRUCTURES

P. Dong and J. Zhang
BATTELLE
Columbus, OH 43201

and

G. Rawls
Westinghouse Savannah River Company
Aiken, SC 29808

ABSTRACT

Detailed residual stress analysis was performed for a multi-pass butt weld, representing the middle butt-girth weld of a storage tank. The analysis procedures took into account representative welding parameters, joint detail, weld pass deposition sequence, as well as temperature-dependent properties. The predicted residual stresses were then considered in stress intensity factor calculations using a three-dimensional finite element alternating model (FEAM) for investigating crack growth behavior for both small elliptical surface and through-wall cracks.

Two crack orientations were considered: one is parallel to the vessel seam weld and the other is perpendicular to the seam weld. Since the longitudinal (parallel to weld) and transverse (perpendicular to weld) residual stresses exhibit drastically different distributions, a different crack growth behavior is predicted. For a small surface crack parallel to the weld, the crack tend to grow more quickly at the surface along the weld rather than into the thickness after some initial growth. The self-equilibrating nature of the transverse residual stress distribution suggests that a through-wall crack parallel to crack cannot be fully developed solely due to residual stress actions. For a crack that is perpendicular to the weld, a small surface crack exhibit a rapid increase in K at the deepest position, suggesting that a small surface crack has the propensity to become a through-wall crack. Once the through crack is fully developed, a significant re-distribution in longitudinal residual stress can be seen. As a result, there exists a limit crack length beyond which further crack growth is deemed unlikely, if there is no external loading.

INTRODUCTION

Fracture mechanics assessment of welds in pressure vessel and piping components often requires knowledge of weld residual stress distributions. In most of codes and recommended practices such as API RP-579 [1] and others [e.g, 2], simplified and conservative distributions were often assumed. For instance, welding-induced residual stresses are often assumed to be tensile, of yield magnitude (or a specified percentage, if post-weld heat treatment applies), and uniform through the thickness. However, over the recent years, there has been a major progress in a better understanding of weld residual stresses, in part, due to the availability of advanced weld residual stress modeling tools [3-4]. It has been demonstrated that the current fitness-for-service procedures can significantly over-estimate the residual stress effects in most cases [3-5] and under-estimate their effects in others [3-5].

In this paper, a detailed case study is reported by considering a typical butt weld in large storage tanks. These tanks were fabricated from steel plates using SMAW and SAW welding techniques. The middle butt-girth welds were made by shielded metal arc welding (SMAW). The tank radius to thickness ratio is 816 to 1. The typical girth weld cross-section and the relevant dimensions are shown in Fig. 1. The girth weld consists of a total of 6 passes, with 3 passes deposited in the inner half of the bevel groove and 3 deposited in the outer half of the groove.

Detailed residual stress analyses were performed using some of the advanced modeling procedures [3-6] to establish representative weld residual stress distribution. Stress intensity factors are then performed using a finite element alternating method (FEAM), as discussed in [7-9], by directly considering the weld residual stress distributions and quasi-static crack growth.

RESIDUAL STRESS ANALYSIS

In the following sections, the full-field residual stress distribution was considered by using some of the advanced finite element analysis procedures as discussed in earlier publications [3-4, 6-7].

2-D Cross-Section Model

A 2-D cross-section of the vessel circumferential butt weld is illustrated in Fig. 1 in which an estimated pass profile for a six-pass weld is also provided. The corresponding finite element model is shown in Fig. 2. Generalized plane strain conditions are used by considering the large radius to wall thickness ratio. The total length (40 inches) of the model was chosen so that the residual stress distributions can be fully contained within the model. Refined elements were used in the weld region for a sufficient resolution in both welding heat flow and residual stress analyses. The boundary conditions for residual stress analysis are also shown in Fig. 2. The prescribed boundary conditions were designed to represent those in a typical multi-pass butt joint for construction of this type. The corresponding residual stress solutions should possess generality for similar joint configurations.

Welding Parameters and Material Properties

The welding parameters used for the residual stress model are listed in Table 1.

Table 1. Welding Parameters for Residual Stress Modeling

Current (I) (amp)	Voltage (V)	Welding Speed (v) (inch/sec)	Electrode Size (inch)	Inter-pass Temperature (^{o}F)	Number of Passes
197.5	24.0	0.125	3/16	50	6

Temperature-dependent thermal-physical properties are used for the welding heat flow analysis. These properties include thermal conductivity and diffusivity. They were obtained from ASME Section II Part D (1998) and assumed the same for both base material A285 and weld metal E6010. Temperature-dependent mechanical properties, i.e., Young's modulus, yield strength, thermal expansion coefficient, and strain hardening information, were inferred from ASME Section II (1998) minimum requirements. The 33.7 ksi value was used for the yield strength of A285 at room temperature in the analysis, while the 56.2 ksi value was used for the yield strength of the filler metal (E6010). The weld metal yield strength overmatches the base material by about 65%. Such weld strength mismatch effects on both residual stresses and fracture behavior can be found in detailed discussions given by Dong and Zhang [10] and Zhang and Dong [11].

Residual Stress Analysis Procedure

As discussed for many similar applications [3,11], the procedure for weld residual stress analysis is typically divided into two parts: transient heat transfer and transient thermo-mechanical analyses. At first, a transient heat transfer analysis solves for the temperature history associated with the heat flow during welding process. Then, the resulting temperature history results are fed into the subsequent transient thermo-mechanical analysis of the nonlinear thermal stress evolution process. Weld residual stresses are the final state of the thermal stresses after all weld passes are completed and the weld is cooled down to the room temperature.

The transient welding heat flow analysis was carried out with the weld passes being deposited sequentially indicated in Fig. 2, using an element activation/deactivation scheme. The subsequent transient thermo-mechanical analysis was carried out using a thermoplasticity analysis procedure along with a weld material constitutive model [3]. With this weld material model, the effects of stress and strain history caused by material melting/re-melting can be properly modeled.

Residual Stress Results

Fig. 3 shows the predicted residual stress distributions. As shown in Fig. 3a, tensile axial (or transverse) residual stresses are present at both inner and outer surfaces near the weld. The tensile stresses at the inner surface are higher than those at the outer surface with the maximum at the weld fusion line. On the outer surface, the maximum transverse stress occurs in the region slightly away from the fusion line. Within the weld cap, the transverse stresses are very low at the outer surface. A high compressive stress zone can be seen in the middle part of the weld section. Fig. 3b shows the corresponding longitudinal (or hoop) residual stress distributions. The longitudinal stresses are dominantly tensile within the weld area except for a small region in the middle section of the weld. The yield strength over-match effects between the base material and weld metal are clearly shown in the longitudinal stress distribution. Because of the overmatch of the filler metal yield strength (65% overmatch), the longitudinal stresses are much higher in the weld region than in the base material nearby. The longitudinal stresses in both regions are beyond their respective yield strengths. It is worth noting that a rather similar residual stress distribution was observed in an early study for a girth weld in reactor core shroud structure [10-11].

Line plots of the as-welded residual stress distributions at the inner, middle, and outer surfaces are shown in Fig. 4. The residual stresses are plotted against the distance from the weld centerline. Fig. 4a shows that the peak transverse stress occurs at the inner surface near the weld fusion line (about 0.25 inch from weld centerline). This is the location where a longitudinal crack (parallel to the weld line) is to be introduced for stress intensity factor calculations in the next section. The magnitude of the peak transverse stress is about 40 ksi at the inner surface. Fig. 4b shows that the longitudinal stresses decay very quickly with the distance from the weld. The longitudinal stresses die

out at the distance of about 0.5 inch away from the centerline on both sides. The magnitude of the peak longitudinal residual stress on the surfaces is about 62 ksi.

Fig. 5a shows the line plots of residual stresses through the plate thickness at the peak transverse stress location (0.25 inch from the weld centerline) and at the weld centerline. The transverse residual stress distributions clearly exhibit a "tension-compression-tension" pattern, i.e., tension at both surfaces and compression in the middle. The longitudinal stresses are dominantly tensile in the entire section except for a small region in the middle of the section.

STRESS INTENSITY FACTOR SOLUTIONS

FEAM Procedure

The finite element alternating method (FEAM) is a convenient numerical method for obtaining stress intensity factor solutions for complex engineering structures [8-9]. The major advantage of this method is that only a finite element mesh of the un-cracked geometry is needed to obtain the stress intensity factors. More importantly, the same mesh can be used to obtain solutions for cracks of many different sizes and geometry. Because the finite element stiffness matrix needs to be reduced only once, regardless of the crack size, location, orientation, etc., the method is extremely efficient. This method is particularly suited for investigating residual stress re-distribution effects on stress intensity factors for a propagating crack under displacement controlled conditions as discussed recently by Dong and Hong [4].

The 3-D finite element model for the un-cracked geometry of the middle-girth weld in this study is shown in Fig. 6 for the stress intensity factor calculations. The 3-D finite element model in Fig. 6 represents half of the flat plate model with a size of 40 inches by 40 inches with the symmetric conditions imposed along the plane at the middle length of the weld, as indicated. The length of the plate was chosen to fully contain residual stress distributions. The finite element mesh was refined in the weld area where the cracks are to be introduced. There are ten elements evenly distributed in the through-thickness direction. The procedure for calculating stress intensity factors involves two steps. First, the as-welded residual stress results from the 2-D residual stress model were mapped onto the 3-D model. Then, through-thickness cracks were considered by means of the FEAM procedure for stress intensity factor calculations.

Two different crack orientations were considered: a transverse crack perpendicular to the weld and a longitudinal crack parallel to the weld. The transverse crack was located in the mid-section of the plate (on the symmetric plane) and the longitudinal crack was located at 0.25 inch away from the weld centerline where the maximum transverse residual stresses are present. Fig. 7a illustrates the orientation and position for the transverse crack (shaded region) modeled using FEAM procedure and Fig. 7b for the longitudinal crack. Five points along the crack front in the thickness direction were chosen for the output of stress intensity factor solutions (Fig. 7c).

Stress Intensity Factor Results

In what follows, small surface cracks are first considered to investigate how a small elliptical surface crack can grow when subjected to the given residual stress field. Then, a through-wall crack of various sizes will be assumed to investigate the crack growth behavior under quasi-static conditions.

Elliptical Surface Cracks

A transverse (perpendicular to weld) surface crack at the butt-girth weld is illustrated in Fig. 8a with respect to the 3D FEAM model and a longitudinal surface crack in Fig. 8b. Under self-similar growth conditions (a/c=2), the corresponding stress intensity factor solutions for a series of crack sizes are summarized in Fig. 8.

As shown in Fig. 8a for the case of a transverse surface crack, when crack size is small (e.g., a=0.2" and c=0.1"), the stress intensity factors along the crack front are relative high along the entire crack front, with highest value at 90^o, dominated by the high tensile longitudinal residual stress field. Under self-similar growth conditions, i.e., a/c=2, the stress intensity factors at the entire crack front initially decreases as the crack size increases until the crack depth (c) extends beyond the mid-thickness (at c > 0.3"). With further increase in crack size (e.g., a>1", c>0.5"), the stress intensity factor at the deepest point (90^o) starts increasing rapidly while the stress intensity factor at the surface (0^o) still decreases. This is consistent with the longitudinal residual stress distribution at the crack plane (Fig. 5). Once a part of the crack front propagates further beyond the mid-thickness, the high longitudinal residual stress close to the inner surface becomes dominant.

As indicated for the case with crack depth of *c* =0.6", the transverse surface crack may grow rapidly within a small angular span near 90^o to form a partial through-wall crack. To further substantiate this point, a separate analysis was performed to examine the stress intensity factor behavior for a = 1.5" and c = 0.75", just as the crack breaks through the inner surface. The results for this case (Case (b) in Fig. 9) is superimposed with those in Fig. 8a and re-plotted in Fig. 9. By comparing the stress intensity results between Cases (a) and (b) in Fig. 9, it can be seen that the K values are elevated along the partial through-wall crack front from about 57^o at the inner surface to 0^o once the surface crack breaks through the inner surface wall.

If a longitudinal crack is oriented along the weld at the inner surface (near the fusion line, Fig. 8b) where high tensile transverse residual stresses are present, the stress intensity factor distributions along the crack front are shown in Fig. 8b. As the crack depth increases, the stress intensity factors decrease rapidly near the deepest positions (near 90^o), while an increase in K can be seen at the surface position (0^o). This can be explained by examining the transverse residual stress distributions in Fig. 5a. As the crack front extends into the mid-thickness region, high compressive stresses become dominant. This suggests that a small longitudinal surface crack is likely to develop into a

shallow and long surface crack and eventually becomes arrested at the mid-thickness region due to the compressive residual stresses.

Through-Wall Cracks

As discussed in the previous section, if a small transverse surface flaw is situated within or near a girth weld, the surface may eventually grow into a through-wall crack. A longitudinal initial surface flaws that are identified potentially to grow in the length direction (parallel to welds), through-wall cracks might still form if a partial through-wall crack length becomes sufficiently long. In such situations, tensile stress states might develop within its remaining ligament for potential growth in the crack depth direction.

A transverse through-wall crack is first considered as illustrated in Fig. 7a.
The stress intensity factor results for the transverse crack are plotted in Fig. 10. Seven different sizes of cracks were analyzed. The crack size ranges from 0.4 inch to 10 inches. The results show that the stress intensity factors are initially high when the crack size is small and decrease rapidly as the crack size increases. The stress intensity factor becomes negative as the crack size reaches 10 inches. In addition, the stress intensity factors are essentially constant along the crack front for all crack sizes except for the smallest one (Fig. 10a). It is worth noting that the stress intensity factors for the crack length (2a) of 2 inches are still at about 20 ksi*in$^{1/2}$ even though the longitudinal residual stress in Fig. 4b at the crack front positions is almost zero. This is due to the re-distribution of the longitudinal residual stress with the presence of a crack, as shown in Fig. 12 for two different crack sizes. In this figure, the longitudinal residual stress distribution before a crack was introduced is shown in dashed lines. As a transverse (perpendicular to the weld direction) crack with half size of a = 0.5" was introduced, the line marked by circle symbols represents the re-distribution of the longitudinal residual stresses obtained directly from the element centroids that are located closest to the crack position in the 3-D FEAM model. (Note that the finite element mesh is rather coarse for approximating the stress results for a given crack location using those at element centroid positions.) Due to the presence of the crack, the longitudinal residual stresses are relieved within the cracked region. This leads to an increase in tensile stresses ahead of crack tip from the original residual stress level before a crack is considered. This trend is clearly shown in Fig. 12.

The stress intensity factor results for the longitudinal cracks are plotted in Fig. 11. Six different sizes of cracks were analyzed. The crack size ranges from 1 inch to 10 inches. For all these crack sizes, the stress intensity factor distributions along the crack front share a similar trend, i.e., being positive near both surfaces and negative in the middle. This is mainly because the transverse stresses are tensile at both surfaces and compressive near the weld mid-thickness. As the crack size increases beyond 2a=4 inches, the magnitude of the stress intensity factors at both middle and outer surfaces become approximately constant, although the values at inner surface decreases only slightly since the longitudinal cracks are subjected to the same transverse residual stress field, regardless of the crack sizes considered.

CONCLUSIONS

Detailed thermo-mechanical residual stress analysis was performed for an idealized multi-pass butt weld, representing the middle butt-girth weld of a storage tank. The analysis procedures took into account representative welding parameters, joint detail, weld pass deposition sequence, as well as temperature-dependent properties. The predicted residual stresses were mapped onto a 3-D finite element alternating model for calculating the stress intensity factors. Both longitudinal and transverse cracks with respect to the weld orientation were considered with crack size (2a) varying from 0.4 to 10 inches. The major findings can be summarized as follows:

(1) Both transverse and longitudinal residual stresses are tensile near the surfaces. The transverse residual stresses become highly compressive near the mid-thickness while the longitudinal residual stresses reduce to near zero at the mid-thickness.

(2) A small transverse to weld surface flaw tends to grow into a surface breaking through-wall crack. Once becoming a through-wall cracks, there exists a length limit beyond which further growth is not likely without external loading. The length limit is related to the longitudinal residual stress distribution.

(3) A small parallel to weld surface flaw, once growing into a certain depth, tends to grow in length direction along a weld in the residual stress field examined. For through-wall cracks, a continued growth in length direction along the weld is not likely without external loading.

Acknowledgement: The authors acknowledge the financial support for this study from Westinghouse Savannah River Company under DOE Subcontract No. AC09467T.

REFERENCES

1. API RP-579, 2000 First Edition, “Recommended Practices for Fitness-for-Service”.

2. PD6493:1991, “Guidance on Methods for Assessing the Acceptability of Flaws in Fusion Welded Structures,” British Standards Institute.

3. Dong, P. and Brust, F.W, “Welding Residual Stresses and Effects on Fracture in Pressure Vessel and Piping Components: A Millennium Review and Beyond,” *The Millennium Issue, ASME Transactions: Journal of Pressure Vessel Technology,* Vol. 122, No. 3, August, pp. 329-328, 2000.

4. Dong, P. and Hong, J.K., “Consistent Treatment of Residual Stresses In Fracture Assessment Solutions,” Proceedings of 2002 ASME Pressure Vessel and Piping

Conference, PVP-Vol. 434 *Computational Weld Mechanics, Constraint, and Weld Fracture*, Vancouver, Canada, August 4-8 2002, pp. 89-100.

5. Bouchard, J. and Bradford, C., "Validated Axial Residual Stress Profiles for Fracture Assessment of Austenitic Stainless Steel Pipe Girth Welds," PVP Vol. 422: *Fracture and Fitness*, Proceedings of ASME PVP Conference, Atlanta, Georgia, U.S.A., July 22-26, 2001.

6. Dong, P., "Residual Stress Analysis of a Multi-Pass Girth Weld: 3D Special Shell Versus Axisymmetric Models," ASME Transaction: *Journal of Pressure Vessel Technology*, Vol. 123, No. 2, 2001, p 207-213.

7. Brust, F.W., Dong, P., and Zhang, J., 1997, "Influence of Residual Stresses and Weld Repairs on Pipe Fracture," ASME Pressure Vessel and Piping Conference Proceedings, PVP-Vol. 347, *Approximate Methods in the Design and Analysis of Pressure Vessel and Piping Components*, pp. 173-191, 1997.

8. Wang, L., Brust, F.W., Atluri, S.N., 1997, "The Elastic-Plastic Finite Element Alternating Methods (EPFEAM) and the Prediction of Fracture under WFD Conditions in Aircraft Structure; Part I: EPFEAM Theory," *Computational Mechanics*, 19(5), pp. 356-369

9. Zhang, J., Dong, P., Brust, F. W., William J. Shack, Michael E. Mayfield, Michael McNeil, 2000. "Modeling Weld Residual Stresses in Core Shroud Structures", Nuclear Engineering and Design, 195, pp. 171-187.

10. Dong, P. and Zhang, J., "Residual Stresses in Strength-Mismatched Welds and Implications on Fracture," *Engineering Fracture Mechanics*, 64, pp. 485-505, 1999.

11. Zhang, J. and Dong, P., "Residual Stresses in Welded Moment Frames and Implications for Structural Performance," *ASCE Journal of Structural Engineering*, Vol. 126, No. 3, March, 2000, pp. 306-315.

12. Dong, P., "Modeling of Weld Residual Stresses and Distortions: Advanced Computational Procedures and Practical Applications," *Keynote Lecture* – Proceedings of The Sixth International Conference on Residual Stresses (ICRS-6), Oxford, United Kingdom, July 10-12, 2000, pp. 1223-1335.

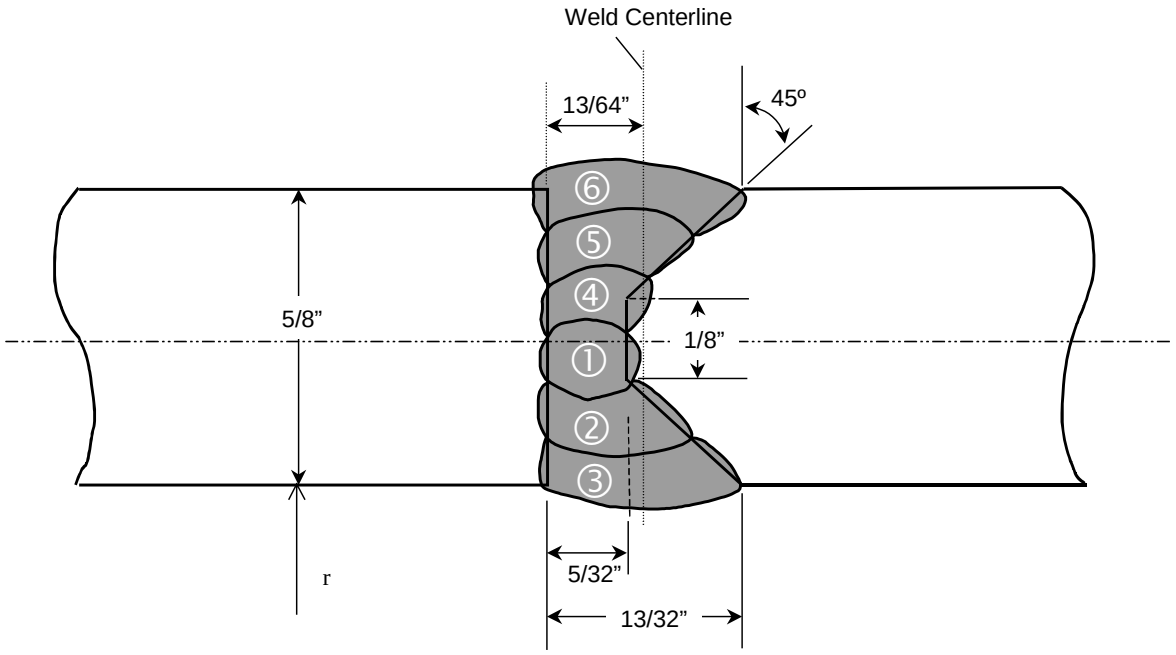

Fig. 1 Geometry and weld-pass profiles for a butt-girth weld in storage tank

(a) Entire Model

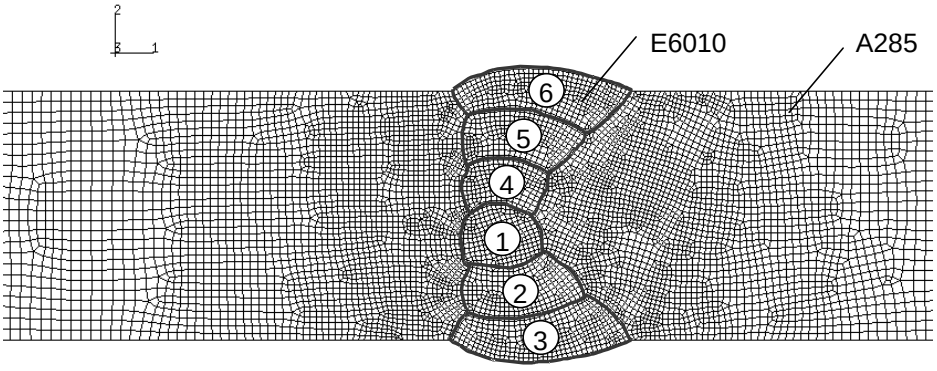

(b) Local View of Weld Region - 6 Passes

Fig. 2 Finite element residual stress model

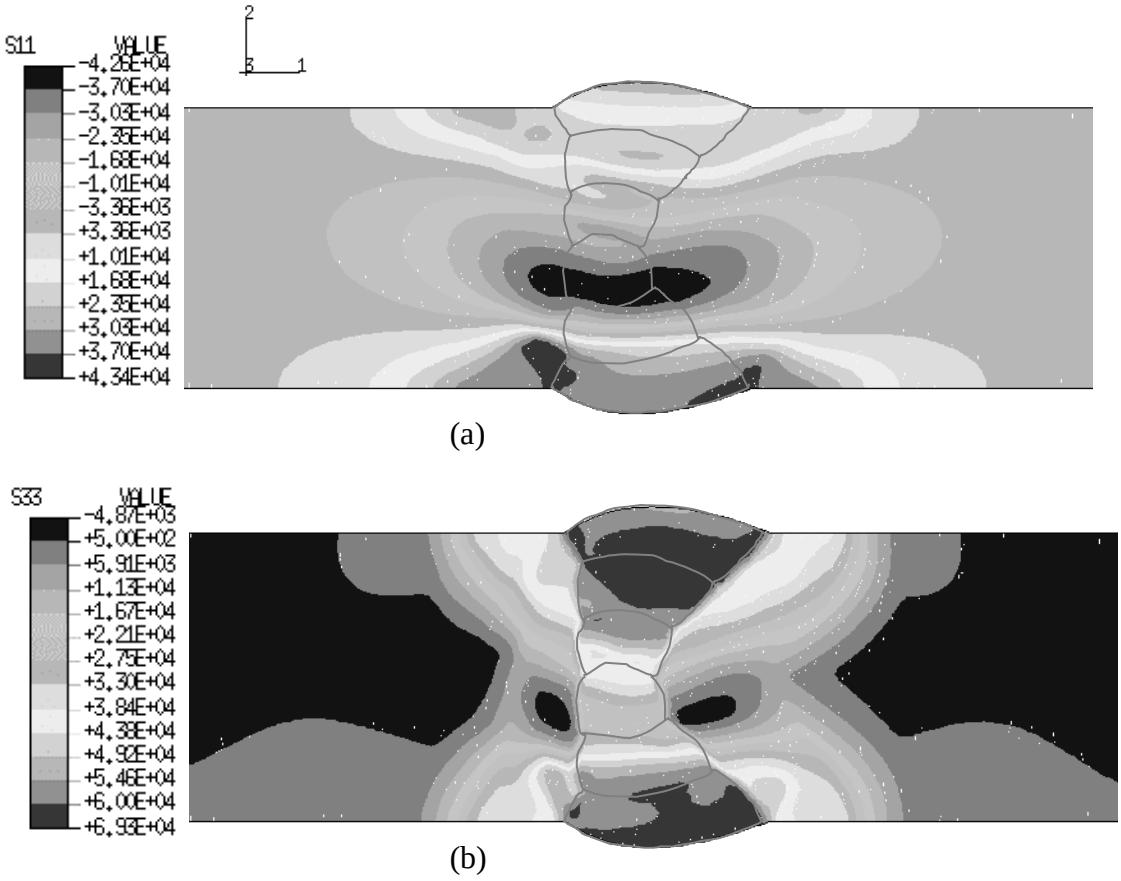

Fig. 3 Predicted weld residual stress distributions: (a) Axial - σ_{11}; (b) Hoop - σ_{33}

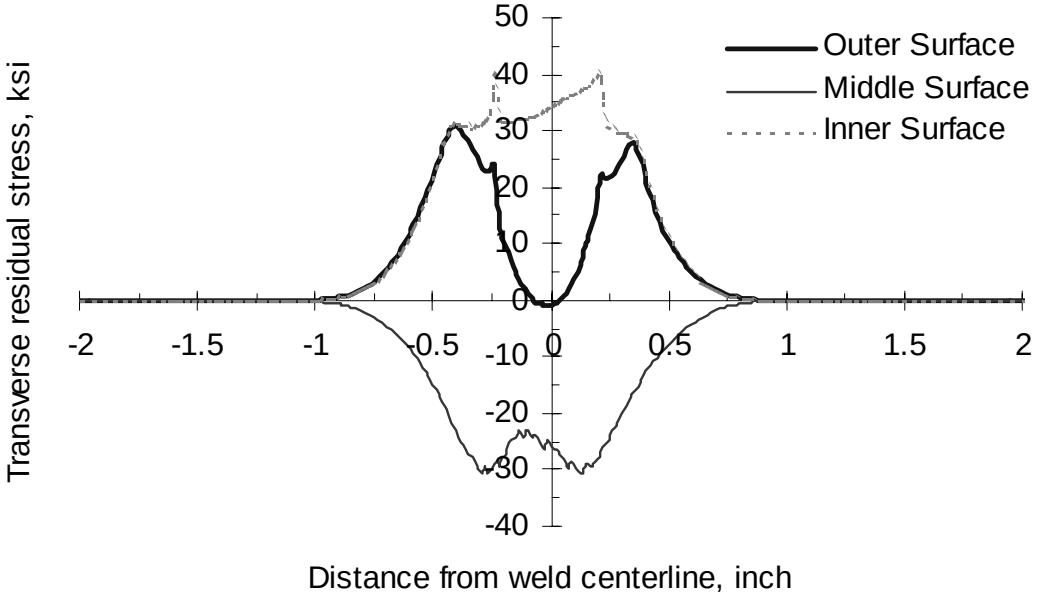

(a)

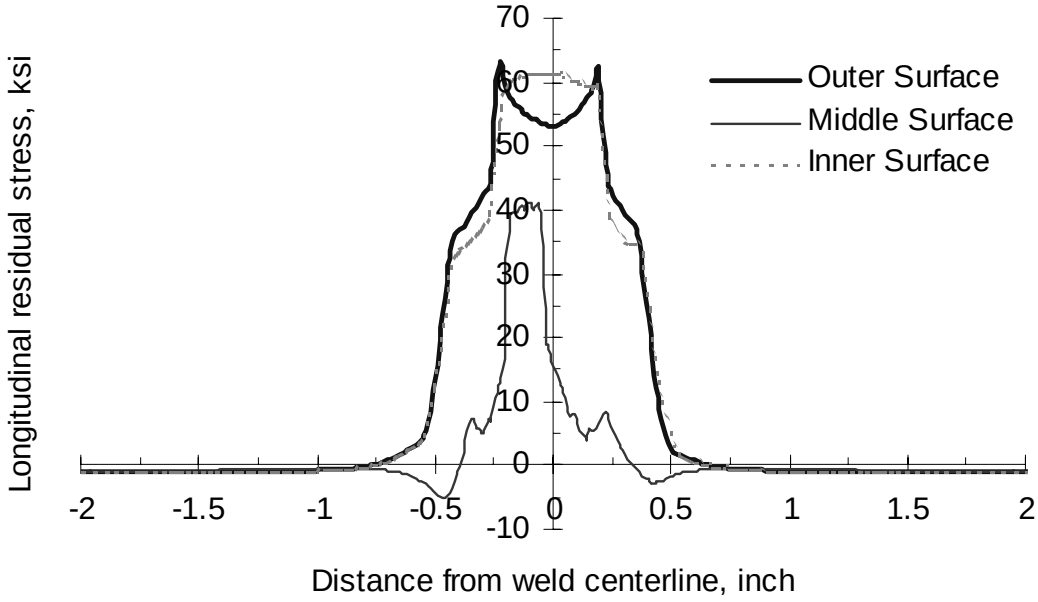

(b)

Fig. 4 Residual stress distributions at inner, middle, and outer surfaces: (a) Transverse residual stress; (b) Longitudinal residual stress

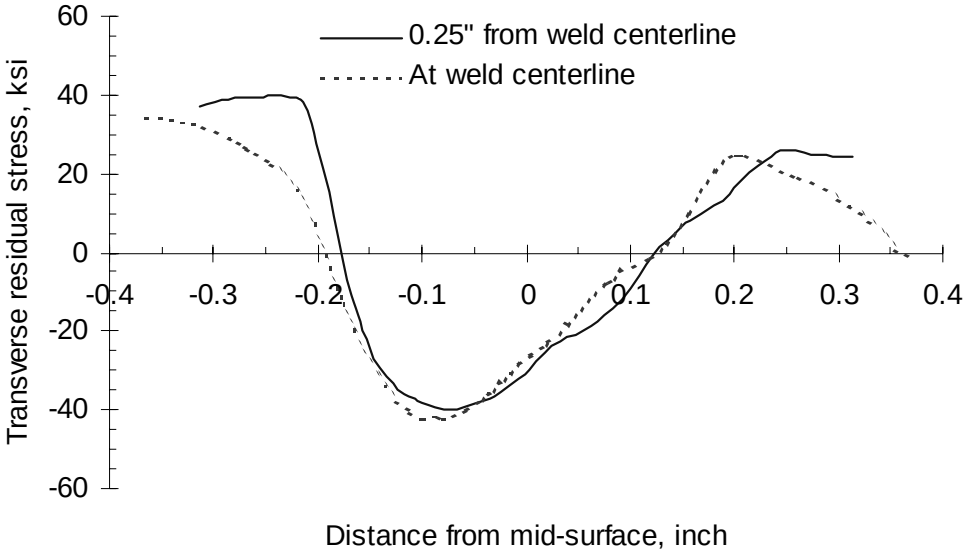

(a)

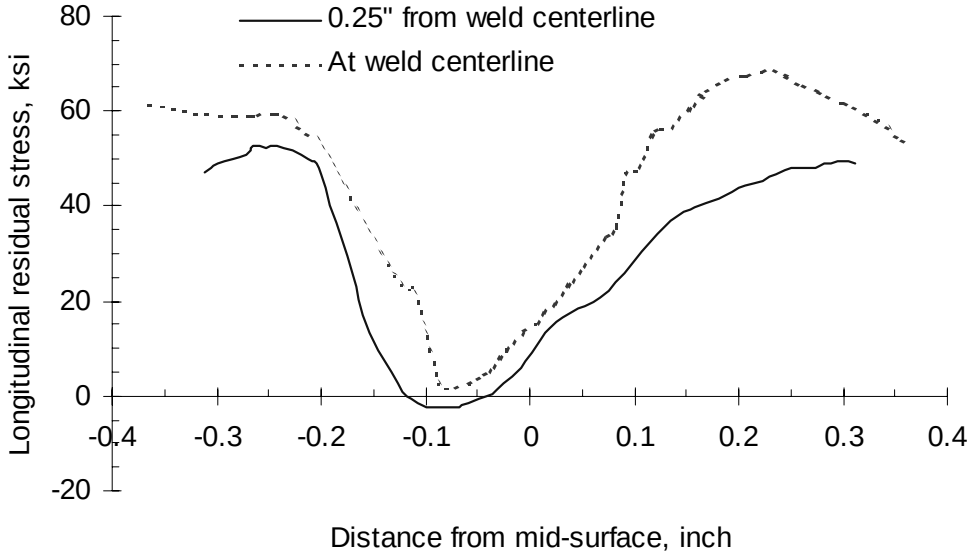

(b)

Fig. 5 Through-wall residual stress distributions: (a) Axial - σ_{11}; (b) Hoop - σ_{33}

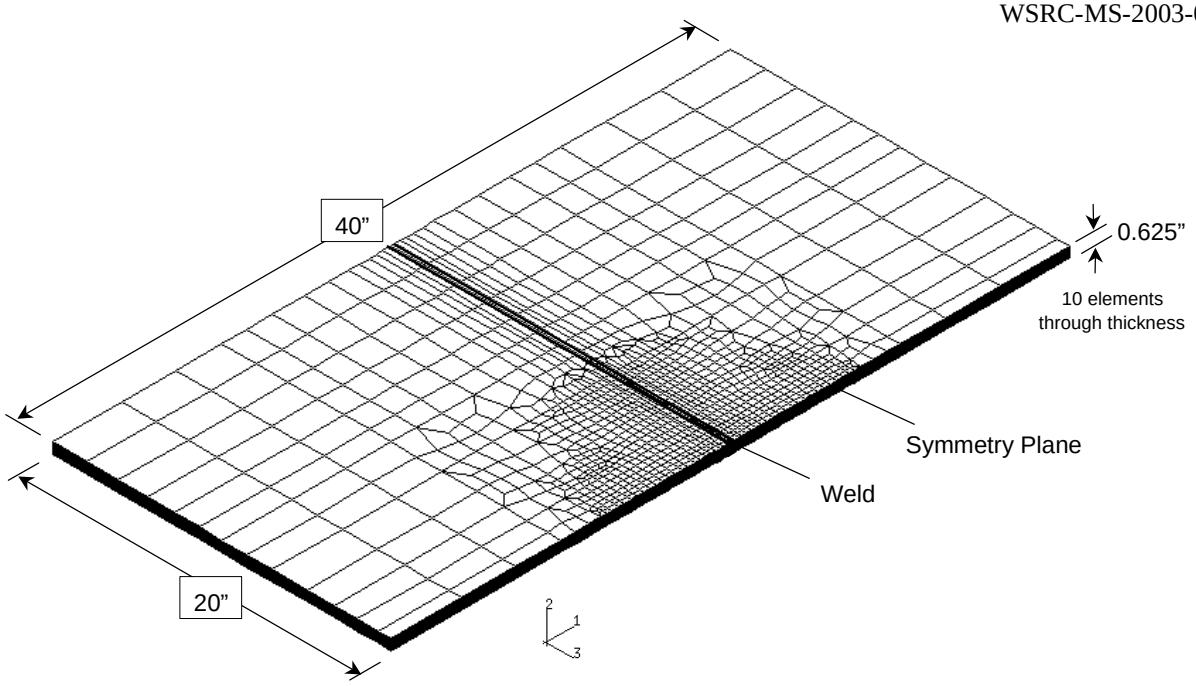

Fig. 6 3-D FEAM model for stress intensity factor solution - half model

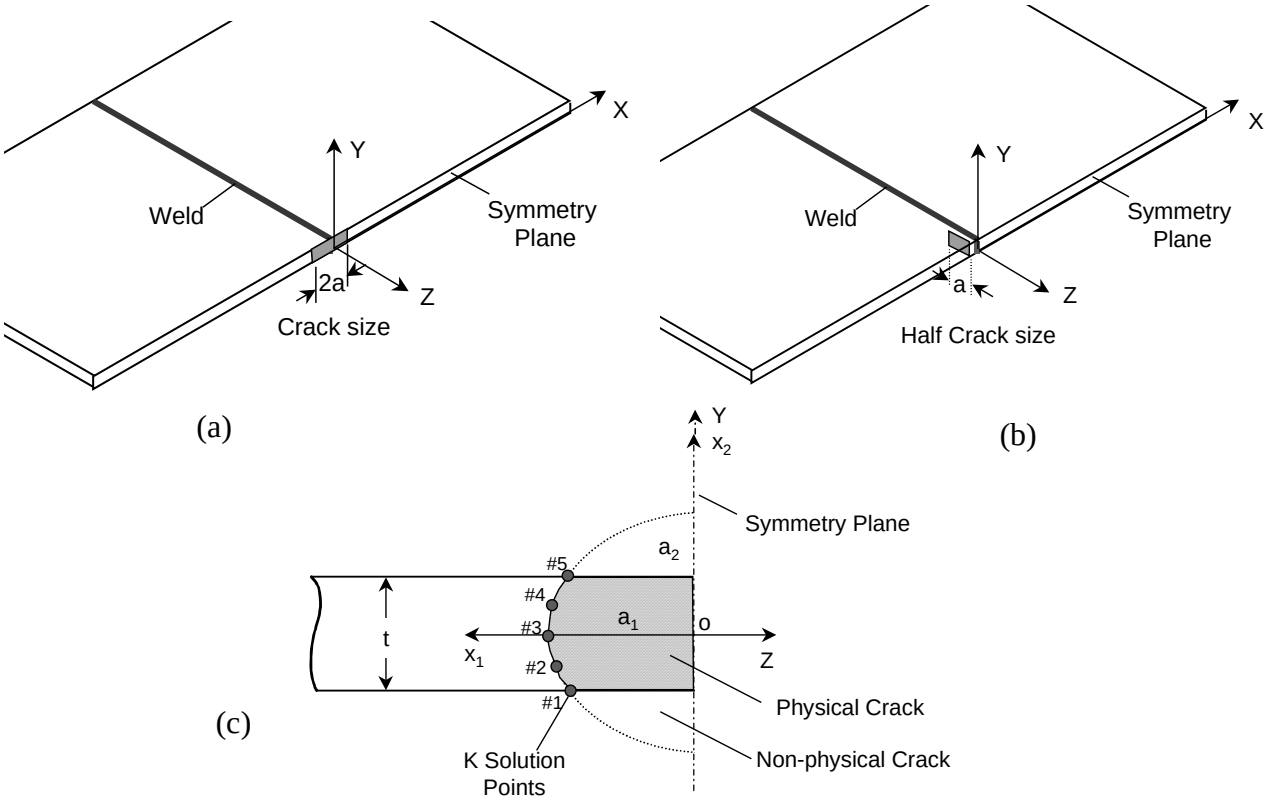

Fig. 7 Through-wall crack orientation and FEAM definition: (a) Crack transverse to weld; (b) crack along weld; (cc) Crack front definition in FEAM

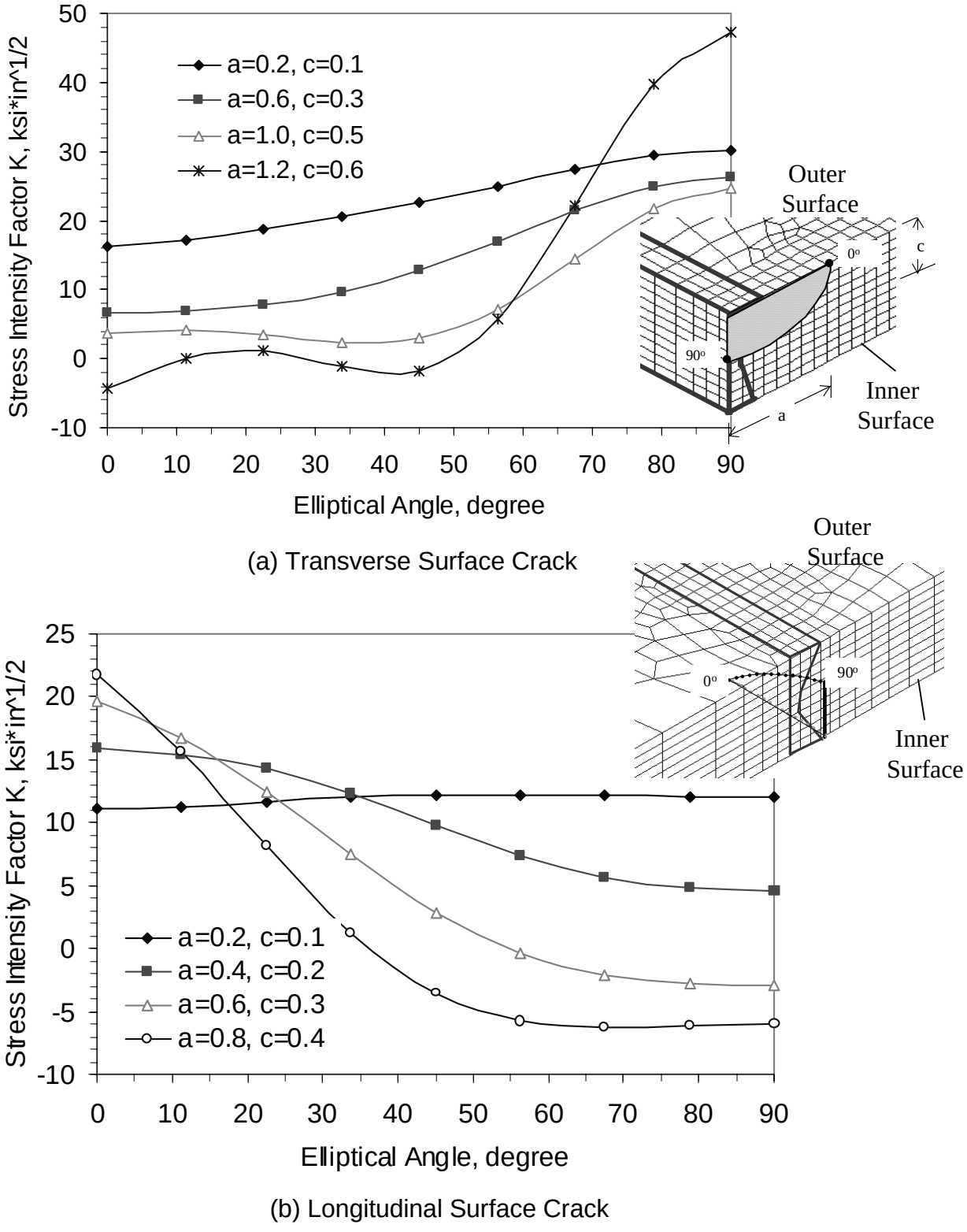

Figure 8. Stress Intensity Factors (K) for Surface Cracks in Butt Girth Weld - Self-Similar Growth (a/c=2)

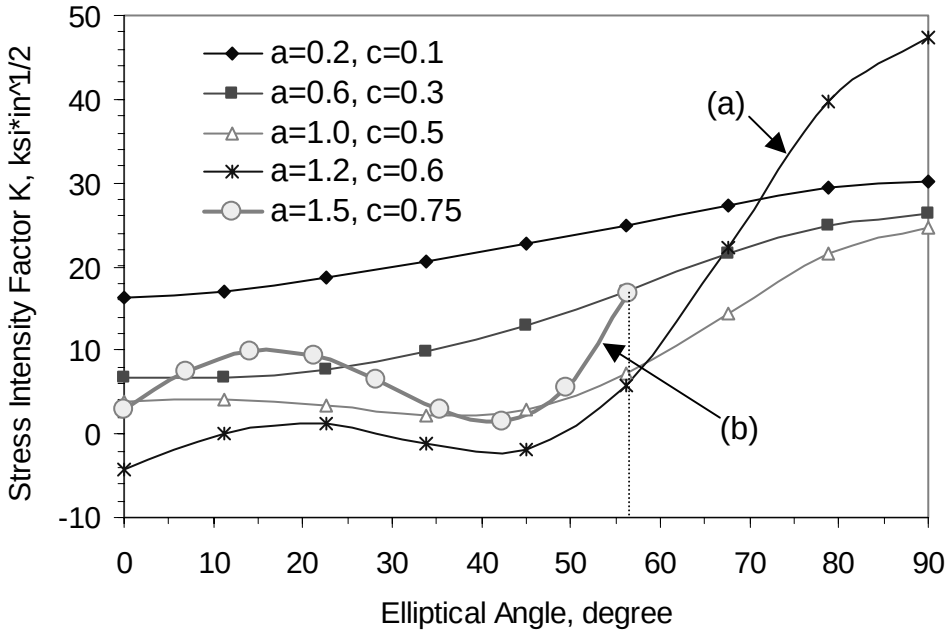

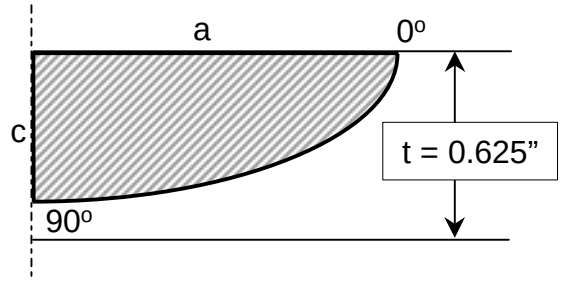

Case (a) Transverse Surface Crack Before Breaking Through Inner Surface

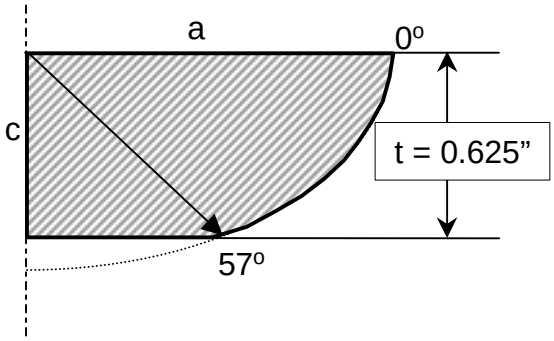

Case (b) Transverse Surface Crack after Breaking Through Inner Surface: Partial-Through Wall Crack

Figure 9. K-Solutions for Transverse Surface and Partial Through-Wall Crack (a/c=2) - Butt Girth Weld

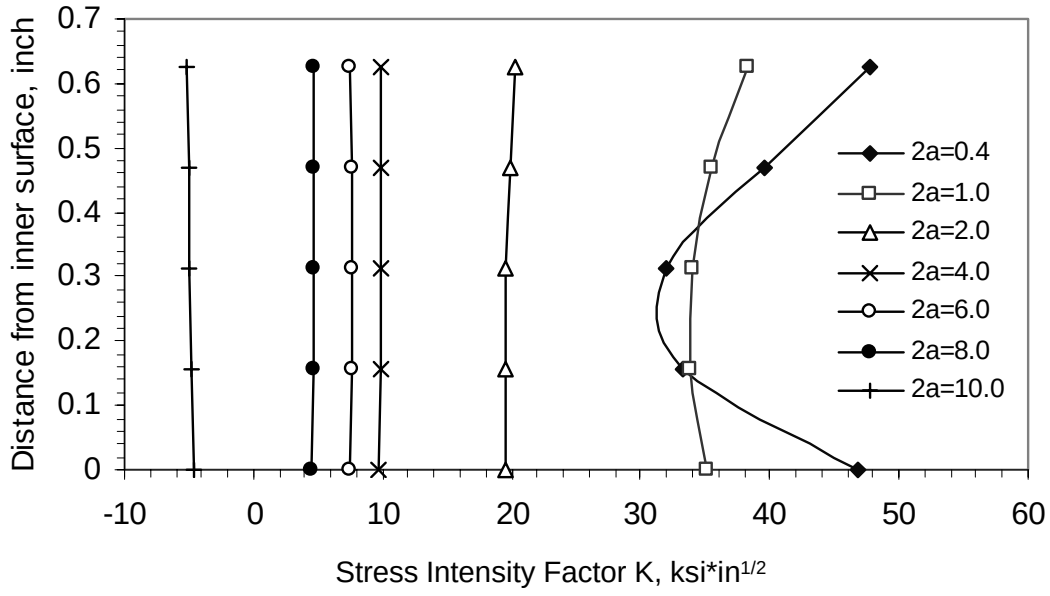

(a)

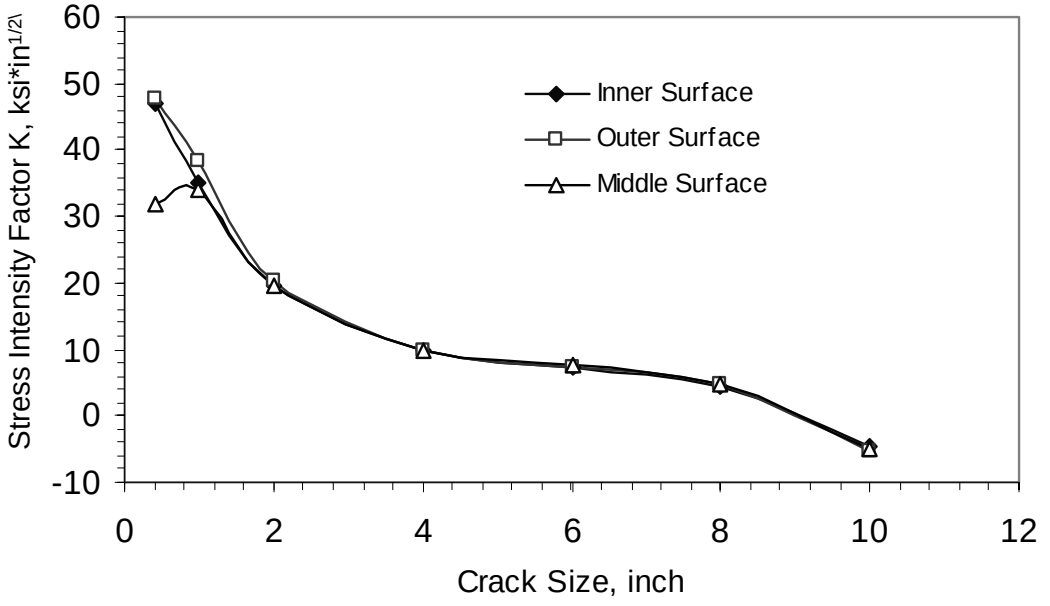

(b)

Fig. 10 K-solutions for transverse crack perpendicular to weld: (a) K versus through-thickness position; (b) K versus crack size (2a)

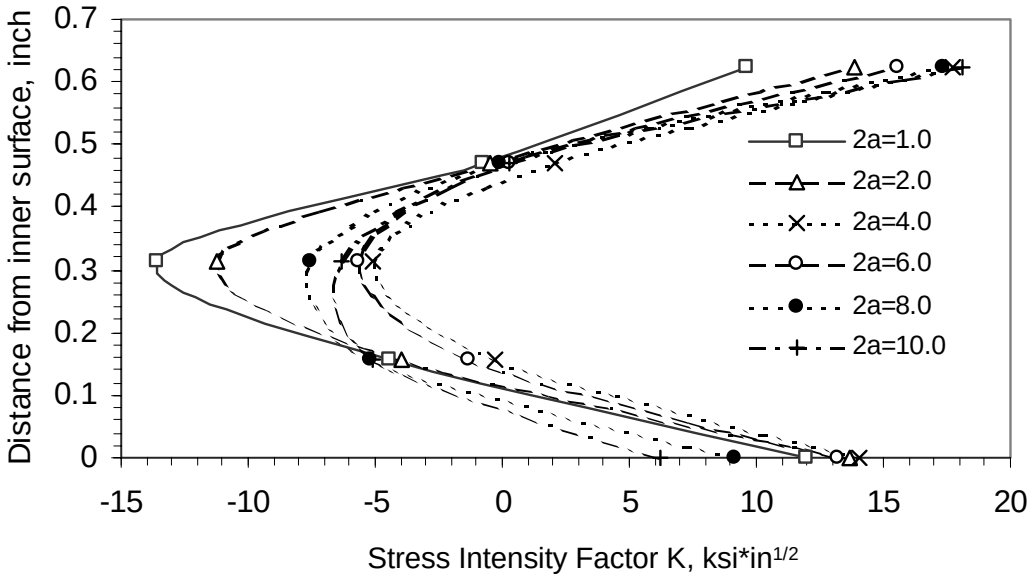

(a)

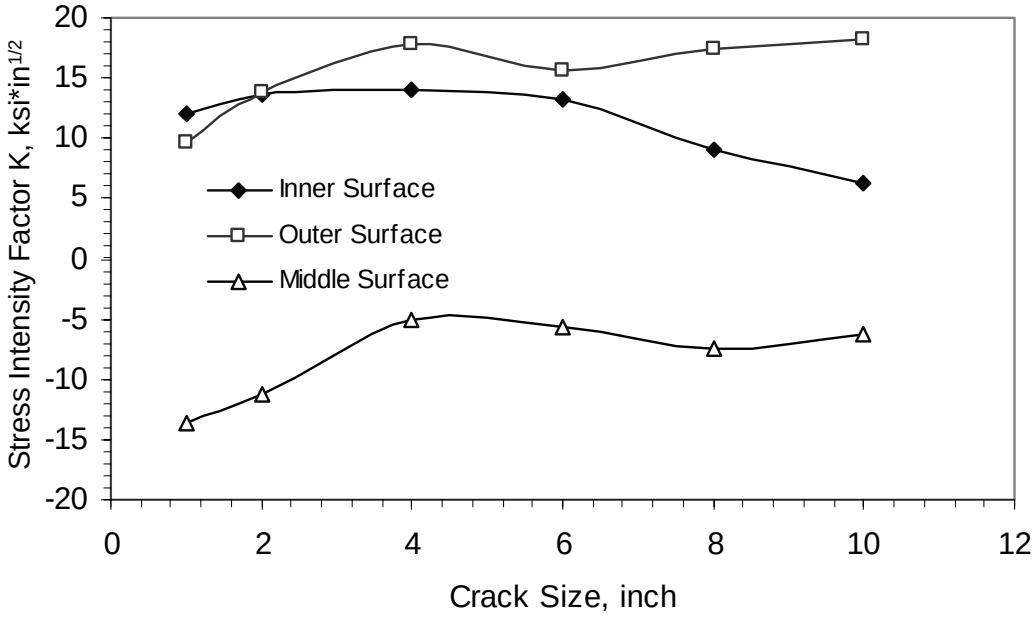

(b)

Fig. 11 K-solutions for longitudinal crack parallel to weld: (a) K versus through-thickness position; (b) K versus crack length (2a)

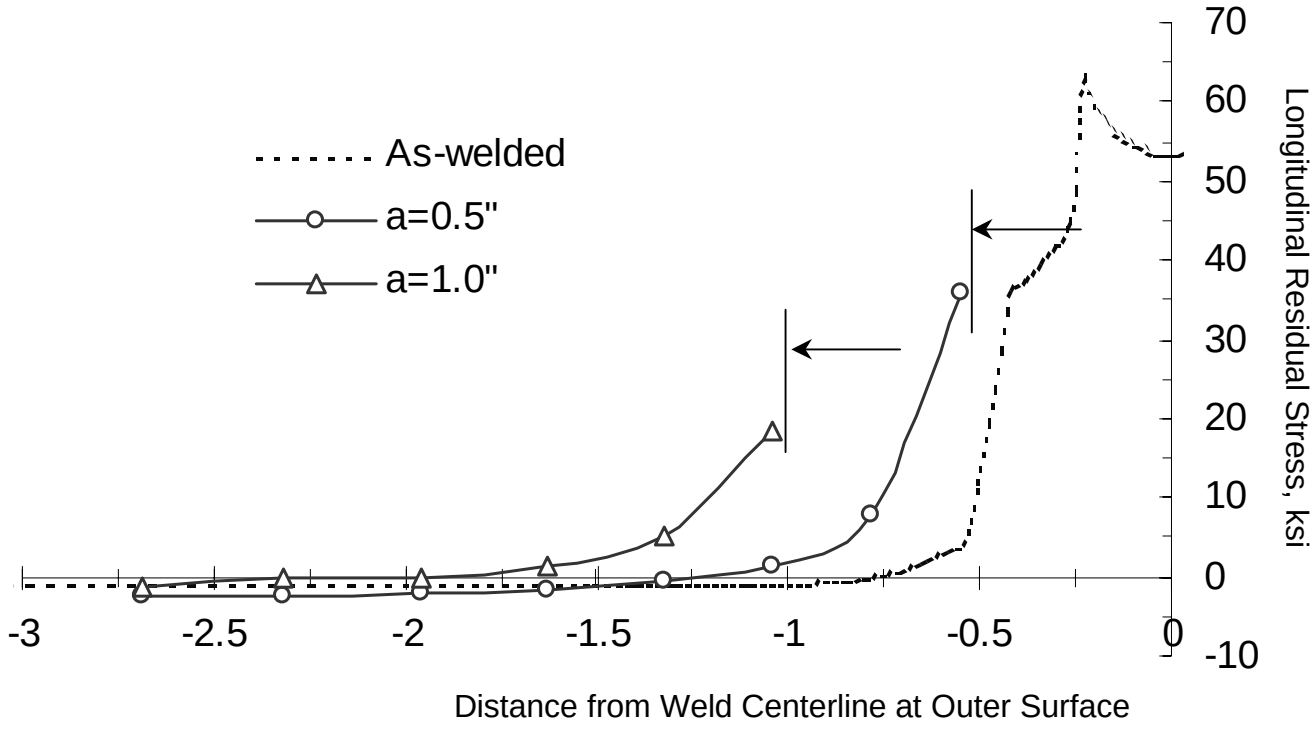

Fig. 12 Residual stress re-distributions ahead of crack front as crack size increases